



HAL
open science

Interplay between electrochemistry and optical imaging: The whole is greater than the sum of the parts

Neso Sojic, Laurent Bouffier

► To cite this version:

Neso Sojic, Laurent Bouffier. Interplay between electrochemistry and optical imaging: The whole is greater than the sum of the parts. *Current Opinion in Electrochemistry*, 2022, 34, pp.101007. <10.1016/j.coelec.2022.101007>. <hal-03853648>

HAL Id: hal-03853648

<https://hal.science/hal-03853648v1>

Submitted on 22 Nov 2022

HAL is a multi-disciplinary open access archive for the deposit and dissemination of scientific research documents, whether they are published or not. The documents may come from teaching and research institutions in France or abroad, or from public or private research centers.

L'archive ouverte pluridisciplinaire HAL, est destinée au dépôt et à la diffusion de documents scientifiques de niveau recherche, publiés ou non, émanant des établissements d'enseignement et de recherche français ou étrangers, des laboratoires publics ou privés.



HAL Authorization

Review Article

Interplay between electrochemistry and optical imaging: The whole is greater than the sum of the parts

*Neso Sojic and Laurent Bouffier**

Address

Univ. Bordeaux, CNRS, Bordeaux INP, Institut des Sciences Moléculaires (ISM), UMR 5255, F-33400 Talence, France

Corresponding author: Bouffier, Laurent (laurent.bouffier@enscbp.fr)

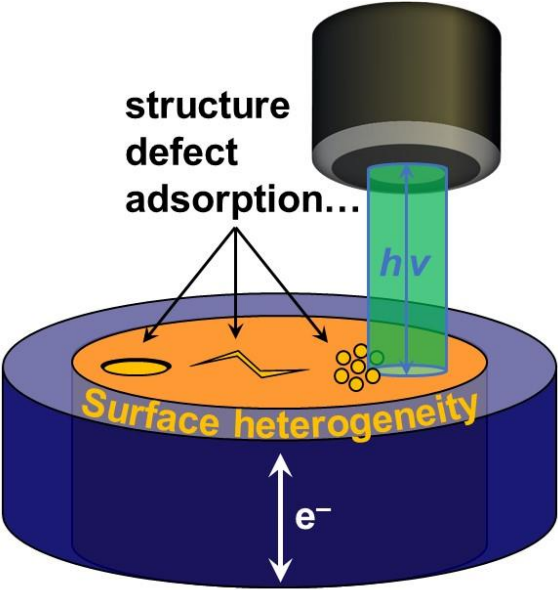
Abstract

Optical techniques can afford a powerful characterization of the solid/liquid interface that is composed of an electrode immersed in an electrolyte. While a typical electrochemical measurement such as current intensity is averaged over the entire electrode surface, the access to surface heterogeneity can provide an increased level of information enabling to rationalize and optimize the performance of chemical or biochemical sensors. In this opinion paper, we will briefly review the different strategies developed to translate an electrochemical process into a luminescence signal. Also, several key examples will be selected and commented in order to highlight the key advantages of coupling electrochemistry with optical imaging, essentially fluorescence and electrochemiluminescence.

Keywords

Opto-electrochemistry; Fluorescence; Confocal laser scanning microscopy; Modified electrode; Electrochemiluminescence

Graphical Abstract



Introduction

In the context of analytical chemistry, electrochemistry offers a wide variety of techniques, methods and strategies to enable a precise determination of a given molecular target. Compared to other approaches, electrochemistry offers a number of advantages such as the possibility to monitor several variables (current, charge, potential, impedance, etc.). However, an intrinsic limitation arises from the use of a solid/liquid interface since the electron transfer process is averaged over the whole electrode surface. That is why a classic electrochemical measurement except scanning electrochemical microscopy (SECM) is blind to surface heterogeneity. However, in most cases, the electrode surface cannot be considered as ideal or defect less. Therefore, the space-resolved mapping of the electrochemical response can play a major role in the development and optimization of modified electrodes for sensing applications.

The combination of electrochemistry with an appropriate imaging technique appears necessary in order to solve such a problem [1],[2],[3],[4]. There are indeed several possibilities but in most cases, a so-called *in situ* coupling is more complicated to be performed in comparison with a sequential characterization (i.e. *ex situ*). This opinion paper will focus on luminescence as a tool to image electrode surfaces. The selected examples are not meant to be exhaustive but the idea is to illustrate key analytical strategies involving wide field microscopy, fluorescence confocal laser scanning microscopy (F-CLSM), [5] or electrochemiluminescence (ECL) imaging [6].

Main text

Electrochemically-induced fluorescence modulation

The goal of this section is to introduce the various strategies that have been proposed in the literature for fluorescence imaging of an electrochemical process. The first approach implies the use of a dye whose fluorescence is modulated at the vicinity of the electrode surface. In most cases, a pH-sensitive fluorescence probe is selected. Fluorescein can be considered as the archetype and was first used in such a context by Engstrom et al. and more recently by many others [7],[8],[9],[10],[11]. In all these examples, a potential step is applied to an electrode surface to enable an electrochemical reaction that either produces or consumes protons such as the $2 e^-$, $2 H^+$ reduction of benzoquinone. Therefore, a pH gradient is promoted at the vicinity of the electrode surface in unbuffered or low-supported buffered solutions. This gradient is revealed by fluorescein, which exhibits a massive increase of brightness ($B = \epsilon \times \phi$, i.e. product of the molar absorptivity and fluorescence quantum yield) between the mono- and dianionic forms ($pK_a = 6.43$, $B = 10,700$ and $71,500 M^{-1} cm^{-1}$, respectively). It is noteworthy that several other pH sensitive dyes have also been reported such as quinine employed to reveal oxygen evolution or oxide formation [12]. More recently, a water-soluble hydroxypyrene derivative (HPTS) was used to visualize the diffusion layer surrounding a carbon fibre microelectrode, [13] or to convert quantitatively an electrochemical current into a fluorescence signal [14].

An alternative strategy is to use a so-called electrofluorogenic probe [15]. It means a redox-active molecule whose fluorescence properties are modulated upon electron transfer. One typical family of molecules that has been widely used during the last decade is phenoxazine. The redox couple composed of resorufin (RF) and resazurin (RZ) is very popular since RZ is mildly fluorescent ($\phi = 0.11$ at pH 10) whereas RF exhibits a much larger quantum yield of 0.41 at the same pH [16]. These molecules have been used to visualize the activity of discrete electrocatalysts, [17] convert an electrochemical response into a fluorescence output, [18],[19] or monitor a diffusion layer [16],[20]. In addition, depending on the necessity to promote a fluorescence enhancement or extinction, several pathways have been proposed. The electrochemical reduction of RZ to RF affords a positive fluorescence signal whereas the subsequent reduction of RF to the colourless dihydroresorufin (DH) results in a fluorescence drop [20],[21]. On the contrary, DH which is unstable and reoxidizes spontaneously in presence of O_2 can be quantitatively generated in solution with an excess of

glucose (i.e. through a homogeneous redox reaction) prior to be electrochemically re-oxidized [18]. A last alternative is offered by Amplex Red, a well-known DH derivative, which is air stable to obtain a fluorescence increase upon an electrochemical oxidation [22]. Following a comparable strategy, the use of several other electrofluorogenic dyes is also possible and was recently reviewed by Buriez and co-workers [23].

Finally, another interesting strategy takes advantage of fluorescence quenching at a metal surface. It was first proposed by Bizzotto et al. and applied to monitor the electrochemical desorption of an organic layer immobilised at the electrode surface [24],[25]. Fluorescence is completely quenched when a dye is localized in close proximity to a bulk metal surface, which is typically the case for thiol self-assembled monolayer (SAM) on a gold electrode. In that case, a fluorescence event can be measured upon an electrochemical desorption when the fluorophore leaves the surface as illustrated in Figures 1a and 1b. In this example, a well-organized SAM is prepared by using a thiol functionalized with a BODIPY (boron-difluoride-dipyromethene) moiety. Prior to desorption, BODIPY fluorescence is quenched whereas a marked increase of fluorescence appears when scanning the potential towards negative values. The maximum fluorescence intensity is monitored at -1.5 V (Fig. 1b) and vanishes at more negative values since the desorbed BODIPY dyes diffuse immediately away from the electrode [26].

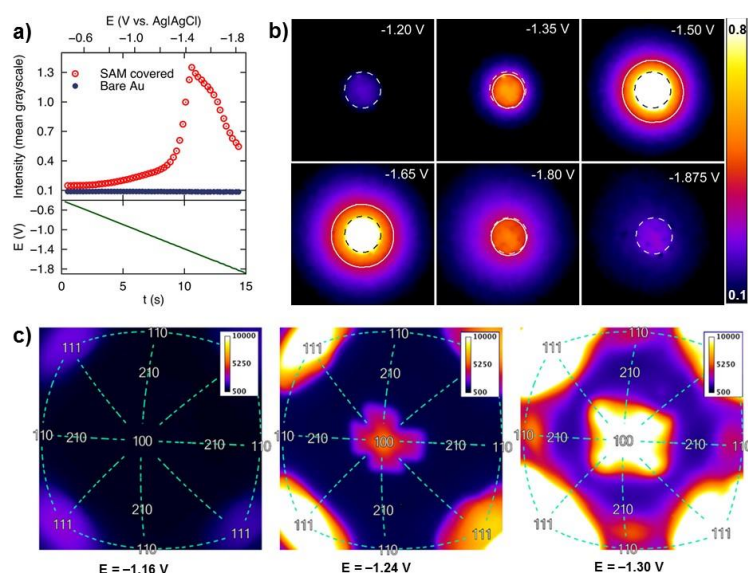


Figure 1. (a) Variation of the fluorescence intensity during a linear potential sweep at a gold electrode modified with a SAM containing a fluorophore. (b) Corresponding fluorescence images at selected potentials during the reductive desorption. Adapted from Ref. [26] with permission from the American Chemical Society, Copyright 2013. (c) Comparable experiment conducted on a single crystal Au bead electrode revealing the stepwise desorption at specific crystallographic planes. Adapted from Ref. [27] with permission from the American Chemical Society, Copyright 2015.

Access to spatial information

One of the first example of F-CLSM imaging was proposed by Unwin and co-workers with benzoquinone used as a redox-active probe and fluorescein acting as reporter [28]. This contribution was rather fundamental and discussed in details the formation of the pH gradient by combining experimental measurements with simulations. However, this method was also applied to image a 4×4 microelectrode array where a faulty electrode can be immediately and unambiguously identified within the array by the absence of surrounding

fluorescence. In a more recent and striking example, Bizzotto and co-workers studied the influence of the surface structure on SAMs prepared with either single or mixed components. Here, the key element is to use a single crystal Au bead electrode enabling to image the complete stereographic triangle (Fig. 1c), [27]. In this example, the reductive desorption of the SAM is again monitored and occurs sequentially starting from 111 planes, prior to 100 and 110 planes on the same electrode but at different spatial localizations. These stepwise reductive desorption potentials follow qualitatively the sequence of the corresponding potential of zero charge that can be measured at low-index faces Au single crystal electrodes [29]. It is noteworthy that in the latter example, the fluorophore was linked covalently to the electrode surface. On the contrary, when the fluorescence arises from a species that is dissolved in solution, the image resolution can be affected by diffusional blurring. In such a context, Compton and co-workers proposed to confine the fluorescence of a pH-sensitive reporter at the direct vicinity of the electrode surface by tuning the concentration of a strong acid such as HClO₄ in solution [30]. This results in improved the images in which the diffusional blurring was significantly reduced.

As stated earlier in the field of biosensors, the surface of a modified electrode cannot be strictly homogenous and many sources of inhomogeneity can therefore be considered such as substrate defects, aggregation or non-specific adsorption [31]. We selected two original studies in order to highlight the added value of fluorescence microscopy to address the homogeneity of electrodes that were modified either by a DNA probe or an enzyme. In the case of DNA biosensors, the interfacial organization of a mixed SAM is directly influenced by the substrate crystallinity as well as the immobilization procedure. For example, DNA concentration is a key parameter since a diluted solution enables a homogeneous layer whereas a more concentrated solution might favour the formation of aggregates (Fig. 2a), [32]. Also, these typical aggregates are persistent and necessitate a more drastic reductive desorption to get removed from the surface as illustrated in Fig. 2b. From this series of experiments, it is clear that a pristine electrode surface can only be regenerated after applying a rather negative potential because milder conditions are insufficient to remove quantitatively these DNA aggregates. Here, the use of fluorescence microscopy definitely helps to interrogate the quality and homogeneity of the DNA layer and might improve the resulting analytical figures of merit.

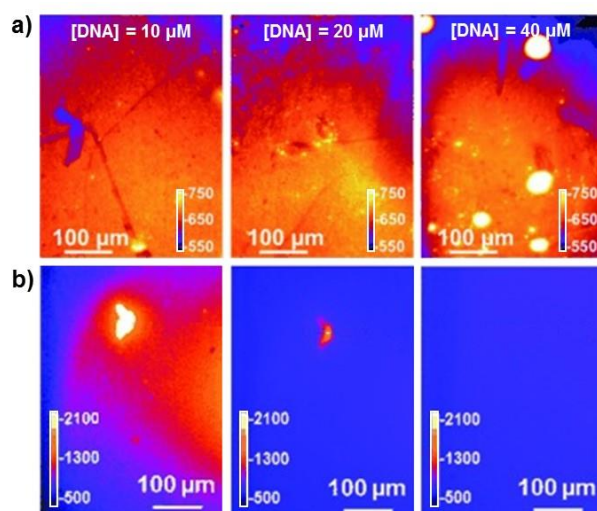


Figure 2. (a) Fluorescence images acquired at open-circuit potential for a polycrystalline gold electrode modified with various concentration of a DNA probe functionalized with a thiol and a BODIPY ends, respectively. (b) Fluorescence images of a mixed SAM of DNA/Mercaptobutanol prepared on a polycrystalline gold electrode acquired before (left) and after reductive desorption ($E = -1.25$ V, middle and $E = -1.40$ V, right). Adapted from Ref. [32] with permission from Wiley-VCH, Copyright 2015.

The optimization of enzyme electrodes remains an essential challenge for the preparation of efficient biosensors, biofuel cells or wearable bioelectronics [33],[34],[35],[36]. Once again, the electrochemical performances are strongly influenced by the homogeneity of the enzyme layer that can be monitored by *in situ* F-CLSM. This was recently exemplified with bilirubin oxidase (BOD) adsorbed at a graphite electrode [37]. BOD drives O₂ reduction together with proton consumption and the corresponding pH gradient is observed with fluorescein dye. Fluorescence imaging provides a direct visualization of surface heterogeneity either in the plane of the electrode (Fig. 3a) or through a 3-dimensional reconstruction by staking images recorded at incremental horizontal positions (Fig. 3b). These images unambiguously revealed the presence of surface defects that drastically affect the local fluorescence intensity. This trend is even more striking at high magnification (Fig. 3c) where the hot spots were assigned to surface micro-holes or cracks originating from the sonication of the electrode after the polishing step. Here, fluorescence microscopy offers a unique way to characterize *in situ* a modified electrode and improve the corresponding fabrication procedure.

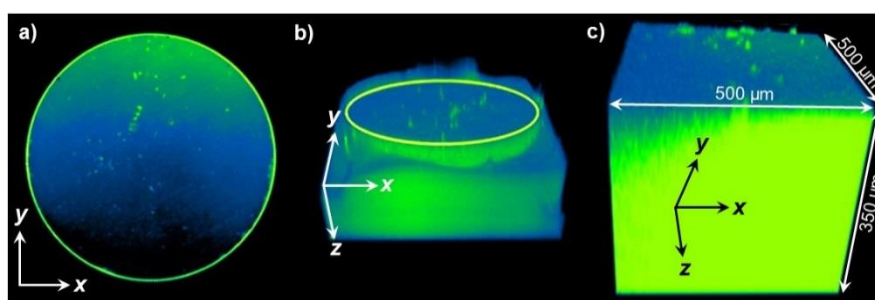


Figure 3. Fluorescence images acquired during O₂ reduction at an enzymatic electrode (bilirubin oxidase, BOD). (a) Representative image recorded in the focal plane. (b) 3D reconstruction (i.e. z-stack) at a constant potential of 0.3 V vs. Ag/AgCl from images recorded at a magnification of $\times 5$. (c) Idem at $\times 20$. The images are displayed with a lookup-table (i.e. the fluorescence intensity appears as a colour gradient from blue to green). Adapted from Ref. [37] with permission from the American Chemical Society, Copyright 2020.

Special case of electrochemiluminescence (ECL)

ECL is a very powerful technique that is widely employed as a readout for various analytical applications [38]. In ECL, the fluorophore is not excited by photon absorption but following a sequence of reactions that is initiated by an electron transfer step. One key advantage of ECL is evidenced when using a combination of several dyes that can be activated either individually or collectively, enabling multiplexed analytical strategies for the simultaneous detection of several analytes [39]. Typically, ECL is promoted by using a sacrificial coreactant that operates either in oxidation or in reduction. Among the most popular coreactant species, tri-propylamine (TPA) and 2-(dibutylamino)ethanol are effective in oxidation whereas benzoyl peroxide or persulfate activates a reductive ECL pathway. However, TPA was reported once to equally act in reduction, which was rather intriguing from a mechanistic point of view [40]. Recently, the use of optical imaging revealed without ambiguity that the corresponding ECL signal originated in fact from the counter electrode (CE) and not from the working electrode (WE) [41],[42]. This is illustrated in Fig. 4 when using [Ru(bpy)₃]²⁺ as red luminophore (Fig. 4a) or Ir(ppy)₃ as green dye (Fig. 4b) in presence of TPA coreactant. In both cases, ECL is solely visible at the CE upon application of a reductive pulse at the WE. Conversely, applying a positive potential step at the WE induces ECL strictly on this electrode [42].

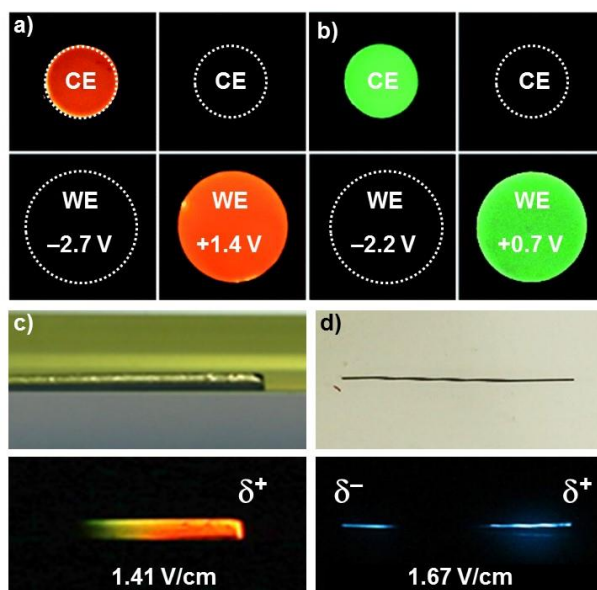


Figure 4. (a) Photographs of the ECL of 5 mM $[\text{Ru}(\text{bpy})_3]^{2+}$ and 10 mM TPA, or (b) 0.2 mM $\text{Ir}(\text{ppy})_3$ and 10 mM TPA at the working electrode (WE) and counter electrode (CE), upon application of different working electrode potentials. Adapted from Ref. [42] with permission from the Royal Society of Chemistry, Copyright 2021. (c) Photographs of space-resolved multicolour ECL with $[\text{Ru}(\text{bpy})_3]^{2+}$ and $\text{Ir}(\text{ppy})_3$ generated alongside a bipolar electrode wire. Adapted from Ref. [43] with permission from Elsevier, Copyright 2017. (d) Simultaneous anodic and cathodic ECL of L-012 luminol derivative visualized at the two extremities of a bipolar electrode wire. Adapted from Ref. [44] with permission from the American Chemical Society, Copyright 2021.

Finally, the last selected examples that will be discussed involved ECL generation at bipolar electrodes, which has become increasingly popular during the last decade [45],[46],[47],[48]. Briefly, bipolar electrochemistry is a wireless approach based on the interfacial polarization of a conducting object submitted to an electric field. In that case, the electrochemical reactivity is distributed along the bipolar electrode with one side behaving as a cathode whereas the other one acts as an anode. Once again, the *in situ* imaging of bipolar electrodes is essential to evidence the local reactivity in space as illustrated in Fig. 4c for multicolour ECL [43]. A Pt wire is immersed in a mixture of 10 mM TPA, 0.5 mM $\text{Ir}(\text{ppy})_3$ and 0.05 mM $[\text{Ru}(\text{bpy})_3]^{2+}$. The top image is recorded under ambient light prior to applying the electric field whereas the bottom one was acquired in the dark when applying 1.41 V/cm. Potential-resolved spectra of the corresponding ECL can reveal the sequential activation of only $\text{Ir}(\text{ppy})_3$ prior to a combination of $\text{Ir}(\text{ppy})_3$ and $[\text{Ru}(\text{bpy})_3]^{2+}$ at higher voltages. However, imaging the anodic part of the bipolar electrode shows that the localization of the red and green emissions is controlled in space since the driving force is maximal at the edge and decreases when moving towards the middle of the bipolar electrode (Fig. 4c, bottom). Another fluorophore that is widely employed for ECL is luminol, which gives a typical blue anodic emission in presence of H_2O_2 coreactant. However, reductive ECL is also mentioned in the literature depending on the nature of the electrode materials [49]. Recently, ECL imaging of a bipolar electrode wire made out of iron shows without ambiguity that the ECL of L-012 luminol derivative can be observed simultaneously in oxidation and in reduction with both extremities of the iron wire exhibiting a blue light (Fig. 4d). A careful analysis of the corresponding image demonstrated that the anodic ECL is slightly more intense and is observed on a longer part of the wire compared to the ECL obtained in reduction [44].

Conclusions

The coupling between an electrochemical measurement and the optical imaging of the electrode surface offers a unique way to study electron transfer processes with an additional spatial information. For that, several strategies can be considered such as the use of redox-active dyes or fluorophores whose properties are modulated by an electrochemical reaction. pH-sensitive luminophores or quenching at close proximity of the electrode surface are possible strategies that are used in this field. Such an electro-optical coupling offers a unique way to improve the quality of the modified electrodes since one can directly get access to surface heterogeneity. The fluorescence signal is largely influenced by surface structuration and defects or can interrogate the level of organization of a given molecular layer. For example, DNA sensors or enzymatic electrodes can be optimized when acquiring images of the electrode *in situ*. Finally, the special case of ECL generated at conventional or bipolar electrodes is also discussed since the combination of an electrochemical stimulus with the exact localization of the ECL event can help understanding mechanistic issues depending on the nature of the luminophore, coreactant and electrode material. In the future, we anticipate that such couplings will become increasingly popular and enable a considerable progress in the methods of fabrication of electrochemical devices for sensing applications. Finally, even if the focus was given to fluorescence and/or ECL transductions, one can note that many other possibilities such as surface plasmon resonance (SPR) imaging, [50],[51] or dark field microscopy [52],[53],[54] can also offer very interesting alternatives.

References and recommended reading

Papers of particular interest, published within the period of review, have been highlighted as:

- Paper of special interest
- Paper of outstanding interest

1. Wang W: **Imaging the chemical activity of single nanoparticles with optical microscopy**. *Chemical Society Reviews* 2018, **47**:2485-2508.
2. Wang Y, Cao Z, Yang Q, Guo W, Su B: **Optical methods for studying local electrochemical reactions with spatial resolution: A critical review**. *Analytica Chimica Acta* 2019, **1074**:1-15.
3. Lozeman JJA, Führer P, Olthuis W, Odijk M: **Spectroelectrochemistry, the future of visualizing electrode processes by hyphenating electrochemistry with spectroscopic techniques**. *Analytst* 2020, **145**:2482-2509.
4. Kanoufi F: **Electrochemistry and Optical Microscopy**. In *Encyclopedia of Electrochemistry*, A.J. Bard (Ed.). <https://doi.org/10.1002/9783527610426.bard030108> 2021:1-80.
5. Bouffier L, Doneux T: **Coupling electrochemistry with in situ fluorescence (confocal) microscopy**. *Current Opinion in Electrochemistry* 2017, **6**:31-37.
6. Zhang J, Arbault S, Sojic N, Jiang D: **Electrochemiluminescence Imaging for Bioanalysis**. *Annual Review of Analytical Chemistry* 2019, **12**:275-295.
7. Engstrom RC, Ghaffari S, Qu H: **Fluorescence imaging of electrode-solution interfacial processes**. *Analytical Chemistry* 1992, **64**:2525-2529.
8. Cannan S, Douglas Macklam I, Unwin PR: **Three-dimensional imaging of proton gradients at microelectrode surfaces using confocal laser scanning microscopy**. *Electrochemistry Communications* 2002, **4**:886-892.
9. Bouffier L, Doneux T, Goudeau B, Kuhn A: **Imaging Redox Activity at Bipolar Electrodes by Indirect Fluorescence Modulation**. *Analytical Chemistry* 2014, **86**:3708-3711.
10. Xu W, Ma C, Bohn PW: **Coupling of Independent Electrochemical Reactions and Fluorescence at Closed Bipolar Interdigitated Electrode Arrays**. *ChemElectroChem* 2016, **3**:422-428.
11. Pande N, Chandrasekar SK, Lohse D, Mul G, Wood JA, Mei BT, Krug D: **Electrochemically Induced pH Change: Time-Resolved Confocal Fluorescence Microscopy Measurements and Comparison with Numerical Model**. *The Journal of Physical Chemistry Letters* 2020:7042-7048.

- An excellent effort towards the challenge of time-resolved fluorescence confocal microscopy.

12. Vitt JE, Engstrom RC: **Imaging of Oxygen Evolution and Oxide Formation Using Quinine Fluorescence.** *Analytical Chemistry* 1997, **69**:1070-1076.
13. Yang M, Batchelor-McAuley C, Kästelhön E, Compton RG: **Reaction Layer Imaging Using Fluorescence Electrochemical Microscopy.** *Analytical Chemistry* 2017, **89**:6870-6877.
14. Djoumer R, Chovin A, Demaille C, Dejous C, Hallil H: **Real-time Conversion of Electrochemical Currents into Fluorescence Signals Using 8-Hydroxypyrene-1,3,6-trisulfonic Acid (HPTS) and Amplex Red as Fluorogenic Reporters.** *ChemElectroChem* 2021, **8**:2298-2307.
15. Miomandre F, Audebert P: *Luminescence in Electrochemistry. Applications in Analytical Chemistry, Physics and Biology*; Springer; 2017.
16. Doneux T, Bouffier L, Goudeau B, Arbault S: **Coupling Electrochemistry with Fluorescence Confocal Microscopy To Investigate Electrochemical Reactivity: A Case Study with the Resazurin-Resorufin Fluorogenic Couple.** *Analytical Chemistry* 2016, **88**:6292-6300.
17. Guerrette JP, Percival SJ, Zhang B: **Fluorescence Coupling for Direct Imaging of Electrocatalytic Heterogeneity.** *Journal of the American Chemical Society* 2013, **135**:855-861.
18. Oja SM, Guerrette JP, David MR, Zhang B: **Fluorescence-Enabled Electrochemical Microscopy with Dihydroresorufin as a Fluorogenic Indicator.** *Analytical Chemistry* 2014, **86**:6040-6048.
19. Djoumer R, Anne A, Chovin A, Demaille C, Dejous C, Hallil H, Lachaud J-L: **Converting Any Faradaic Current Generated at an Electrode under Potentiostatic Control into a Remote Fluorescence Signal.** *Analytical Chemistry* 2019, **91**:6775-6782.
- [Proof-of-principle of the quantitative conversion of an electrochemical current into a fluorescence measurement at the counter electrode.](#)
20. de Poulpiquet A, Goudeau B, Garrigue P, Sojic N, Arbault S, Doneux T, Bouffier L: **A snapshot of the electrochemical reaction layer by using 3 dimensionally resolved fluorescence mapping.** *Chemical Science* 2018, **9**:6622-6628.
21. Guerret-Legras L, Audibert JF, Ojeda IMG, Dubacheva GV, Miomandre F: **Combined SECM-fluorescence microscopy using a water-soluble electrofluorochromic dye as the redox mediator.** *Electrochimica Acta* 2019, **305**:370-377.
22. Lefrançois P, Vajrala VSR, Arredondo IB, Goudeau B, Doneux T, Bouffier L, Arbault S: **Direct oxidative pathway from amplex red to resorufin revealed by in situ confocal imaging.** *Physical Chemistry Chemical Physics* 2016, **18**:25817-25822.
23. Guille-Collignon M, Delacotte J, Lemaître F, Labbé E, Buriez O: **Electrochemical Fluorescence Switch of Organic Fluorescent or Fluorogenic Molecules.** *The Chemical Record* 2021, **21**:1-11.
24. Bizzotto D, Pettinger B: **Fluorescence Imaging Studies of the Electrochemical Adsorption/Desorption of Octadecanol.** *Langmuir* 1999, **15**:8309-8314.
25. Shepherd JL, Kell A, Chung E, Sinclair CW, Workentin MS, Bizzotto D: **Selective Reductive Desorption of a SAM-Coated Gold Electrode Revealed Using Fluorescence Microscopy.** *Journal of the American Chemical Society* 2004, **126**:8329-8335.
26. Casanova-Moreno JR, Bizzotto D: **What Happens to the Thiolates Created by Reductively Desorbing SAMs? An in Situ Study Using Fluorescence Microscopy and Electrochemistry.** *Langmuir* 2013, **29**:2065-2074.
27. Yu ZL, Casanova-Moreno J, Guryanov I, Maran F, Bizzotto D: **Influence of Surface Structure on Single or Mixed Component Self-Assembled Monolayers via in Situ Spectroelectrochemical Fluorescence Imaging of the Complete Stereographic Triangle on a Single Crystal Au Bead Electrode.** *Journal of the American Chemical Society* 2015, **137**:276-288.
- [Demonstration that the local structure on a gold bead single crystal electrode does strongly affect the corresponding electrochemical reactivity.](#)
28. Rudd NC, Cannan S, Bitziou E, Ciani I, Whitworth AL, Unwin PR: **Fluorescence Confocal Laser Scanning Microscopy as a Probe of pH Gradients in Electrode Reactions and Surface Activity.** *Analytical Chemistry* 2005, **77**:6205-6217.
29. Doneux T, Steichen M, De Rache A, Buess-Herman C: **Influence of the crystallographic orientation on the reductive desorption of self-assembled monolayers on gold electrodes.** *Journal of Electroanalytical Chemistry* 2010, **649**:164-170.
30. Pruchyathamkorn J, Yang M, Amin HMA, Batchelor-McAuley C, Compton RG: **Imaging Electrode Heterogeneity Using Chemically Confined Fluorescence Electrochemical Microscopy.** *Journal of Physical Chemistry Letters* 2017, **8**:6124-6127.

31. Bizzotto D, Burgess IJ, Doneux T, Sagara T, Yu H-Z: **Beyond Simple Cartoons: Challenges in Characterizing Electrochemical Biosensor Interfaces.** *ACS Sensors* 2018, **3**:5-12.
32. Meunier A, Triffaux E, Bizzotto D, Buess-Herman C, Doneux T: **In Situ Fluorescence Microscopy Study of the Interfacial Inhomogeneity of DNA Mixed Self-Assembled Monolayers at Gold Electrodes.** *ChemElectroChem* 2015, **2**:434-442.
33. Mano N, de Poulpiquet A: **O₂ Reduction in Enzymatic Biofuel Cells.** *Chemical Reviews* 2018, **118**:2392-2468.
34. Kim J, Jeerapan I, Sempionatto JR, Barfidokht A, Mishra RK, Campbell AS, Hubble LJ, Wang J: **Wearable Bioelectronics: Enzyme-Based Body-Worn Electronic Devices.** *Accounts of Chemical Research* 2018, **51**:2820-2828.
35. Zigah D, Lojou E, de Poulpiquet A: **Micro- and Nanoscopic Imaging of Enzymatic Electrodes: A Review.** *ChemElectroChem* 2019, **6**:5524-5546.
36. Dutta S, Patil R, Dey T: **Electron transfer-driven single and multi-enzyme biofuel cells for self-powering and energy bioscience.** *Nano Energy* 2022, **96**:107074.
37. Tassy B, Dauphin AL, Man HM, Le Guenno H, Lojou E, Bouffier L, de Poulpiquet A: **In Situ Fluorescence Tomography Enables a 3D Mapping of Enzymatic O₂ Reduction at the Electrochemical Interface.** *Analytical Chemistry* 2020, **92**:7249-7256.
- [First application of fluorescence confocal microscopy to image an enzymatic electrode *in situ*.](#)
38. Bouffier L, Sojic N: **Chapter 1 Introduction and Overview of Electrogenerated Chemiluminescence.** In *Analytical Electrogenerated Chemiluminescence: From Fundamentals to Bioassays*. Edited by: The Royal Society of Chemistry; 2020:1-28.
39. Hogan CF, Francis PS, Doeven EH: **Chapter 8 Multicolour Electrochemiluminescence.** In *Analytical Electrogenerated Chemiluminescence: From Fundamentals to Bioassays*. Edited by: The Royal Society of Chemistry; 2020:200-246.
40. Cao W, Xu G, Zhang Z, Dong S: **Novel tris(2,2'-bipyridine)ruthenium(ii) cathodic electrochemiluminescence in aqueous solution at a glassy carbon electrode.** *Chemical Communications* 2002:1540-1541.
41. Theakstone AG, Doeven EH, Conlan XA, Dennany L, Francis PS: **'Cathodic' electrochemiluminescence of [Ru(bpy)₃]²⁺ and tri-n-propylamine confirmed as emission at the counter electrode.** *Chemical Communications* 2019, **55**:7081-7084.
- [Optical imaging of ECL experiments reveals that extra-care should be taken with emission originating from the counter electrode.](#)
42. Adamson NS, Theakstone AG, Soulsby LC, Doeven EH, Kerr E, Hogan CF, Francis PS, Dennany L: **Emission from the working and counter electrodes under co-reactant electrochemiluminescence conditions.** *Chemical Science* 2021, **12**:9770-9777.
43. Li H, Bouffier L, Arbault S, Kuhn A, Hogan CF, Sojic N: **Spatially-resolved multicolor bipolar electrochemiluminescence.** *Electrochemistry Communications* 2017, **77**:10-13.
44. Feng M, Dauphin AL, Bouffier L, Zhang F, Wang Z, Sojic N: **Enhanced Cathodic Electrochemiluminescence of Luminol on Iron Electrodes.** *Analytical Chemistry* 2021, **93**:16425-16431.
45. Karimian N, Hashemi P, Afkhami A, Bagheri H: **The principles of bipolar electrochemistry and its electroanalysis applications.** *Current Opinion in Electrochemistry* 2019, **17**:30-37.
46. Bouffier L, Manojlovic D, Kuhn A, Sojic N: **Advances in bipolar electrochemiluminescence for the detection of biorelevant molecular targets.** *Current Opinion in Electrochemistry* 2019, **16**:28-34.
47. Rahn KL, Anand RK: **Recent Advancements in Bipolar Electrochemical Methods of Analysis.** *Analytical Chemistry* 2021, **93**:103-123.
48. Bouffier L, Zigah D, Sojic N, Kuhn A: **Bipolar (Bio)electroanalysis.** *Annual Review of Analytical Chemistry* 2021, **14**:65-86.
49. Håkansson M, Jiang Q, Suomi J, Loikas K, Nauma M, Ala-Kleme T, Kankare J, Juhala P, Eskola JU, Kulmala S: **Cathodic electrochemiluminescence at double barrier Al/Al₂O₃/Al/Al₂O₃ tunnel emission electrodes.** *Analytica Chimica Acta* 2006, **556**:450-454.
50. Shan X, Patel U, Wang S, Iglesias R, Tao N: **Imaging Local Electrochemical Current via Surface Plasmon Resonance.** *Science* 2010, **327**:1363-1366.
51. Hasheminejad M, Fang Y, Li M, Jiang Y, Wang W, Chen H-Y: **Plasmonic Imaging of the Interfacial Potential Distribution on Bipolar Electrodes.** *Angewandte Chemie International Edition* 2017, **56**:1629-1633.
52. Brasiliense V, Clausmeyer J, Dauphin AL, Noël J-M, Berto P, Tessier G, Schuhmann W, Kanoufi F: **Opto-electrochemical In Situ Monitoring of the Cathodic Formation of Single Cobalt Nanoparticles.** *Angewandte Chemie International Edition* 2017, **56**:10598-10601.

53. Yang M, Batchelor-McAuley C, Barton S, Rickaby REM, Bouman HA, Compton RG: **Opto-Electrochemical Dissolution Reveals Coccolith Calcium Carbonate Content.** *Angewandte Chemie International Edition* 2021, **60**:20999-21006.
54. Xie R-C, Batchelor-McAuley C, Yang M, Compton RG: **Substrate mediated dissolution of redox active nanoparticles; electron transfer over long distances.** *Nano Research* 2022, **15**:429-437.